

## **Supplementary Data**

### **Supplementary figure legends**

#### **Figure S1. Type I IFN production after poly(I:C) treatment or transfection in human SV40-fibroblasts**

SV40-fibroblasts from two healthy controls (C1 and C3, indicated with blue and red bars, respectively) were stimulated with extracellular poly(I:C) for 3 hours or by Lipofectamine-mediated transfection with poly(I:C) for 6 hours. The expression of the various subtypes of type I IFN was quantified by RT-qPCR. The *IFN* expression levels shown are expressed relative to *GUS*. The mRNAs for IFNA2, IFNA4, IFNA5, IFNA6, IFNA7, IFNA8, IFNA10, IFNA16, IFNA17, IFNK, and IFNW1 were not detectable under the conditions used. Data from biological triplicates are shown.

#### **Figure S2. Virus-induced IFN production in TLR3 signaling-deficient fibroblasts**

**(A)** ELISA-based determinations of IFN- $\lambda$  production 24 hours after VSV WT or M51R infection at the indicated MOI in control and TLR3 signaling-deficient SV40-fibroblasts. **(B)** Measurement of IFN- $\lambda$  production by ELISA, 24 hours after VSV WT or M51R infection at a MOI of 1, in control or TLR3 signaling-deficient fibroblasts. **(C)** *IFNL1* mRNA levels in fibroblasts without virus infection, or after VSV M51R infection at a MOI of 0.01 for 16 h. The error bars indicate the standard error of the mean of biological triplicates from three independent experiments. *P* values were obtained by one-way ANOVA and subsequent tukey's multiple comparison tests

**Figure S3. The RIG-I-MAVS pathway is intact in TLR3 pathway-deficient cells and mediates the innate immune sensing of VSV M51R**

**(A)** SV40-fibroblasts from a control (C1), UNC-93B<sup>-/-</sup> and NEMO<sup>-/-</sup> patients were transduced with lentiviruses to express control shRNAs (scr: scramble) and shRNAs targeting RIG-I (shRIG-I). The upper panels show western blots probed with an antibody against RIG-I (upper band, \* indicates a non-specific band). The bottom panel shows IFN- $\beta$  production levels, as measured by ELISA after 24 hours of stimulation with extracellular poly(I:C), Lipofectamine-transfected poly(I:C) (poly(I:C) + LPF), RIG-I specific ligand (7sk-as) or VSV WT and M51R at a MOI of 1.

**(B)** SV40-fibroblasts from C1, UNC-93B<sup>-/-</sup> and NEMO<sup>-/-</sup> patients were transduced with control lentivirus and lentivirus expressing shRNAs targeting MAVS (shMAVS). The upper panels show western blots probed with antibodies against MAVS. The bottom panel shows IFN- $\beta$  production levels, as measured by ELISA after 24 h of stimulation with extracellular poly(I:C), Lipofectamine-transfected poly(I:C) (poly(I:C) + LPF), RIG-I specific ligand (7sk-as) or VSV WT and M51R at a MOI of 1.

**(C)** ELISA determination of IFN- $\beta$  production 24 hours after stimulation with poly(I:C) (extracellular), 7sk-as (transfected), uninfected Vero cell RNA (extracellular or transfected), or various amounts of RNA (0.01, 0.1 and 1  $\mu$ g) isolated from Vero cells infected with VSV WT or M51R.

**(D)** ELISA determination of IFN- $\beta$  production 24 hours after infection with VSV WT, M51R or both (WT+M51R) at a MOI of 1.

**(E)** C1, TLR3<sup>-/-</sup>, and UNC93B<sup>-/-</sup> fibroblasts were infected with VSV WT at a MOI of 0.1 for 6 hours and 24 hours, VSV-G RNA was then detected by RT-qPCR.

**(F)** Detection of IFNB mRNA production by RT-qPCR, following 6 hours or 24 hours of infection with VSV WT at a MOI of 1. The error bars indicate standard deviation of biological triplicates from three independent experiments. *P* values were obtained by

one-way ANOVA and subsequent tukey's multiple comparison tests. **(G)** Measurement of IFN- $\beta$  production by ELISA, 24 hours after stimulation with poly(I:C), or infection with VSV WT or M51R with or without inactivation by ultraviolet irradiation (UV), at a MOI of 1.

**Figure S4. Unrestricted virus growth in fibroblasts with TLR3 signaling deficiencies**

**(A-B)** Control fibroblasts (C1~C4) and TLR3<sup>-/-</sup>, UNC93B<sup>-/-</sup>, NEMO<sup>-/-</sup>, STAT1<sup>-/-</sup>, and STAT2<sup>-/-</sup> fibroblasts were infected with VSV WT **(A)** and M51R **(B)** at a MOI of 0.01 for 16 h. Viral VSV-G RNA levels were then determined by RT-qPCR. **(C)** Control fibroblasts (C1~C4) and TLR3<sup>-/-</sup>, UNC93B<sup>-/-</sup>, NEMO<sup>-/-</sup>, STAT1<sup>-/-</sup>, and STAT2<sup>-/-</sup> fibroblasts were infected with or HSV-1-GFP at a MOI of 0.01 for 16 h. HSV-1 *ICP27* RNA levels were then quantified by RT-qPCR. **(D-E)** *IFNB* and *IFNL1* production levels in control and TLR3<sup>-/-</sup>, STAT1<sup>-/-</sup> fibroblasts without virus infection, or after HSV-1 infection for 8 h, 16 h or 24 h, at a MOI of 1. The error bars indicate standard deviations of biological triplicates.

**Figure S5. Low basal levels of IFN- $\beta$  and ISGs in TLR3-deficient human fibroblasts**

**(A)** VSV replication levels in C1, C3 and TLR3<sup>-/-</sup> fibroblasts without IFN- $\alpha$  treatment (NT), treated with IFN- $\alpha$  at the time of viral infection, or treated with IFN- $\alpha$  for 18 hours before viral infection (pretreatment). **(B)** IFN- $\beta$  levels from cultured supernatants of SV40-fibroblasts were measured in the Simoa assay. **(C)** mRNA levels of *IFNB*, *IFNL1*, *CXCL10* and *IFI44L* (relative to GUS) in unstimulated fibroblasts from healthy controls (C1-C6) and TLR3<sup>-/-</sup>, IRAK4<sup>-/-</sup> or MYD88<sup>-/-</sup> individuals, as quantified by RT-qPCR with normalization against average value of controls. Representative data from three independent experiments are shown. P values were obtained for ratio *t* tests by comparing fibroblasts from patients with control fibroblasts (B-C), and the *P* value

is indicated. The error bars indicate standard deviations of triplicate measurements. **(D)** Gene expression profiles for all ISGs obtained with total cell RNA-Seq data from primary fibroblasts from STAT1<sup>-/-</sup> (blue bar) and TLR3<sup>-/-</sup> (orange bar) patients, relative to mean expression in controls. The heatmap shows log fold-changes in ISG expression, with red indicating upregulation and green downregulation.

**Figure S6. Low levels of IFN in conditioned medium from healthy controls rescue the decrease in ISG expression and restrict viral replication in TLR3<sup>-/-</sup> and UNC93B<sup>-/-</sup> cells**

**(A)** Low levels of type III IFN receptor expression in human SV40-fibroblasts. RNA was extracted from SV40-fibroblasts from controls or a TLR3<sup>-/-</sup> patient and analyzed, by RT-qPCR, for the expression of type I IFN (*IFNAR1*, *IFNAR2*) and type III IFN (*IFNLRI*) receptors. The values obtained are expressed relative to GAPDH. **(B)** HSV-1 titer in TLR3<sup>-/-</sup> (left panel) and UNC93B<sup>-/-</sup> (right panel) fibroblasts after pretreatment with conditioned medium (as indicated in parentheses) for 18 h and infection with HSV-1 for 24 h. The error bars indicate the standard error of the mean of biological triplicates. **(C)** Induction of ISGs in UNC-93B<sup>-/-</sup> SV40-fibroblasts grown on glass coverslips and cultured together with conditioned medium from patient or healthy control fibroblasts (as indicated in parentheses) for 18 hours. **(D)** VSV M51R titer in UNC-93B<sup>-/-</sup> fibroblasts after pretreatment for 18 hours with culture medium from healthy control (C1), UNC-93B<sup>-/-</sup> or STAT1<sup>-/-</sup> fibroblasts in the presence or absence of IFN-β-neutralizing antibodies (IFN-β NAb) or an isotype control. **(E)** Levels of mRNA for ISGs (MxA, RIG-I, MDA5, IRF7 and IRF3) in C1 (left panel), UNC-93B<sup>-/-</sup> (middle panel) or STAT1<sup>-/-</sup> (right panel) SV40-fibroblasts, quantified after 18 h of stimulation, as in **(D)**. ISG mRNA levels are expressed relative to GUS mRNA levels.

**Figure S7. RNA-Seq analysis of primary MEFs and VSV challenge at an early time point**

(A) Gene expression profile for all ISGs in *Tlr3*<sup>-/-</sup> MEFs relative to the WT control, as assessed by RNA-Seq. (B) Venn diagram of the ISGs differentially expressed in *TLR3*<sup>-/-</sup> human samples and *TLR3*<sup>-/-</sup> mouse samples. (C, D) WT and *Tlr3*<sup>-/-</sup> MEFs were infected with VSV WT (C) or VSV M51R (D) for 5 hours at the indicated MOI, and VSV-G RNA levels were then quantified by RT-qPCR. The error bars indicate standard deviations of technical triplicates.

**Figure S8. Role of TLR3 in antiviral immunity in cortical and trigeminal neurons**

(A) HPS cell-derived cortical neurons were treated with 1000 IU/mL IFN- $\alpha$ 2b for 24 h and whole cell lysates were analyzed by western blotting. (B) iPSC-derived TG neurons for a control and a *TLR3*<sup>-/-</sup> patient were stained for neuronal (TUJ1), placodal (SIX1), and peripheral sensory neuron (ISL1) markers after 30-50 days of differentiation (upper panels). iPSC-derived cortical neurons from both genotypes stained for neuronal (TUJ1) and forebrain (PAX6 and TBR1) markers (lower panels). No difference was seen in differentiation potential between genotypes for either TG or cortical neurons. (C-D) *IFNB* (C) and *IFNLI* (D) production levels in control and *TLR3*<sup>-/-</sup>, *STAT1*<sup>-/-</sup> iPSC-derived cortical neurons without virus infection, or after HSV-1 infection for 8 h, 16 h or 24 h, at a MOI of 1. (E-G) iPSC-derived trigeminal neurons from a control line, a *TLR3* KO line, and a *TLR3*<sup>-/-</sup> patient line were infected with VSV WT (E) VSV M51R (F) and HSV-1 (G) for the times indicated. Viral replication was assessed in TCID<sub>50</sub> assays. (C-G) The error bars indicate the standard deviations of biological replicates from two (C,D) or three (E-G) independent experiments.

**Figure S9. Downregulation of basal ISGs in TLR3-deficient cortical neurons**

(A) Gene expression profile for all ISGs in TLR3<sup>-/-</sup> (orange bar) and STAT1<sup>-/-</sup> (blue bar) patient-specific iPSC-derived cortical neurons relative to mean expression levels in cortical neurons derived from three control lines, as assessed by RNA-Seq. (B) Gene expression profile for all ISGs in TLR3 KO iPSC-derived cortical neurons relative to levels in cortical neurons derived from the parental control iPSC line. (C-D) Venn diagram of the downregulated (C) or upregulated ISGs (D) differentially expressed in TLR3<sup>-/-</sup> patient iPSC-derived cortical neurons, TLR3 KO iPSC-derived cortical neurons and TLR3<sup>-/-</sup> patient fibroblasts.

**Table S1. List of ISGs differentially expressed in TLR3- and STAT1-deficient human fibroblasts**

Gene expression (including logFC, *p*-value) for the merged list of ISGs differentially expressed in STAT1<sup>-/-</sup> and TLR3<sup>-/-</sup> patient primary fibroblasts, relative to mean expression levels in control cells, with the logFC value color-coded from green (negative value for downregulation) to red (positive value for upregulation) to indicate the magnitude of the change in gene expression. In this table, genes are also labeled to indicate differential expression in STAT1<sup>-/-</sup> or TLR3<sup>-/-</sup> patients.

**Table S2. DAVID GO enrichment analysis for ISGs differentially expressed in human TLR3- and STAT1-deficient fibroblasts**

Gene ontology enrichment (*p*-value < 0.05) for the downregulated differentially expressed ISGs common to STAT1<sup>-/-</sup> and TLR3<sup>-/-</sup> patients.

**Table S3. List of ISGs differentially expressed in *Tlr3*<sup>-/-</sup> MEF cells**

Gene expression fold changes for the ISGs differentially expressed in  $Tlr3^{-/-}$  MEF cells relative to mean levels of expression in WT cells.

**Table S4. ISGs downregulated in human TLR3<sup>-/-</sup> fibroblasts and *Tlr3*<sup>-/-</sup> MEF cells**

**Table S5. GO enrichment analysis for ISGs differentially expressed in *Tlr3*<sup>-/-</sup> MEF cells**

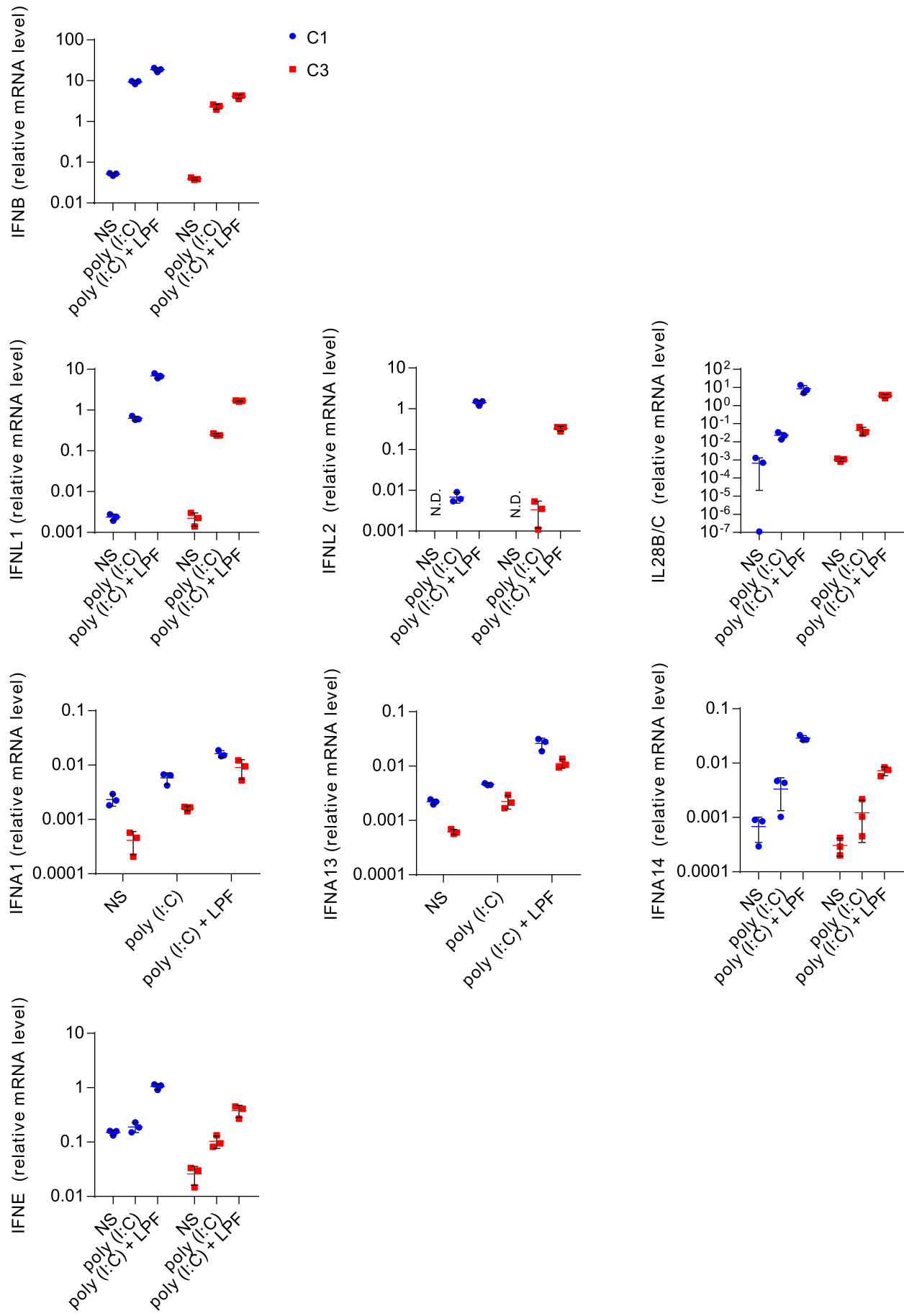
Gene ontology enrichment ( $p$ -value < 0.05) of the downregulated ISGs differentially expressed in  $Tlr3^{-/-}$  MEF cells.

**Table S6. List of ISGs differentially expressed in STAT1<sup>-/-</sup>, TLR3<sup>-/-</sup>, and TLR3 KO iPSC-derived cortical neurons**

Gene expression values and gene ontology enrichment for the ISGs differentially expressed, obtained by contrasting STAT1<sup>-/-</sup> or TLR3<sup>-/-</sup> iPSC-derived cortical neurons with controls, or TLR3 KO iPSC-derived cortical neurons with neurons derived from the parental control line, respectively.

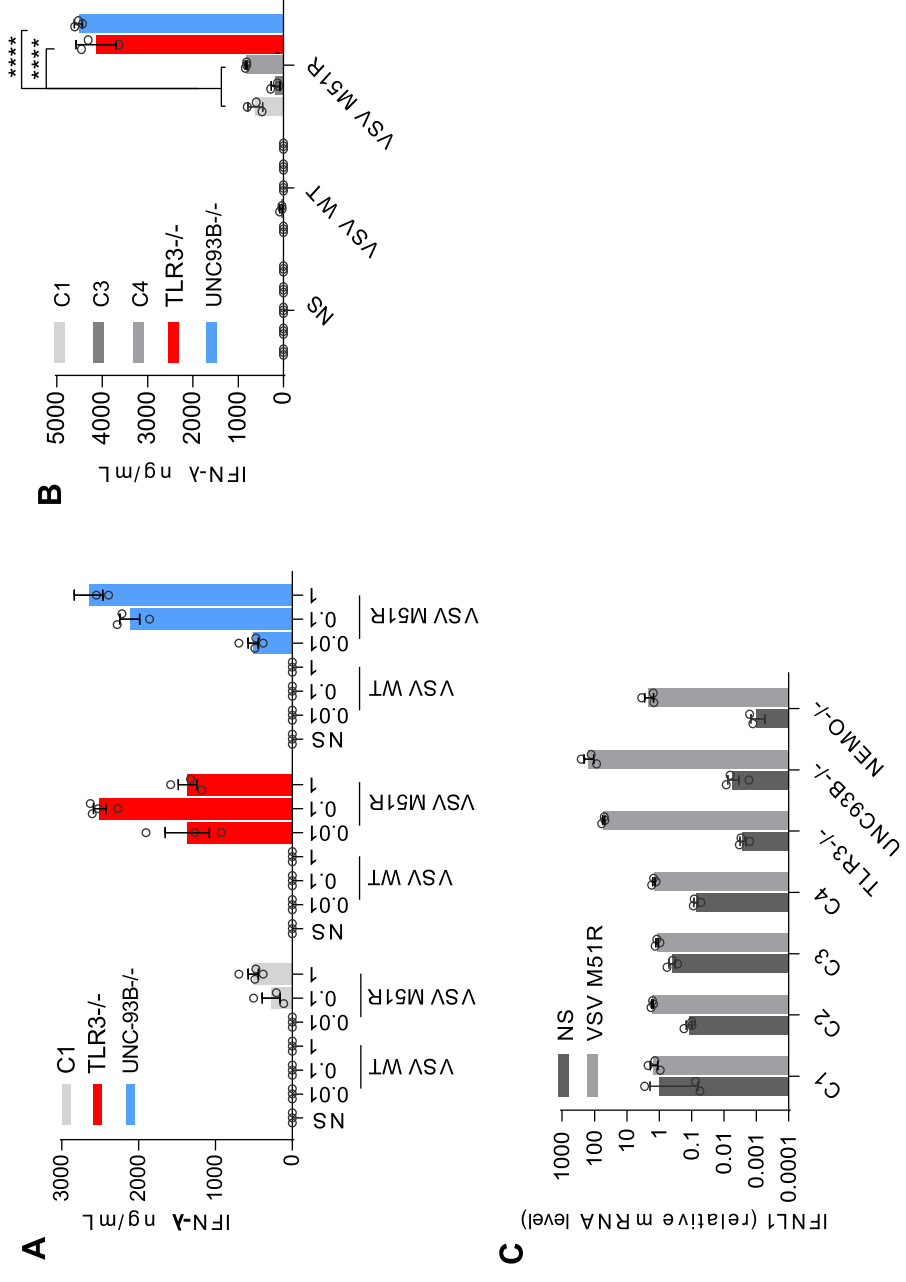
**Table S7. GO enrichment analysis for ISGs differentially expressed in STAT1<sup>-/-</sup>, TLR3<sup>-/-</sup>, and TLR3 KO iPSC-derived cortical neurons**

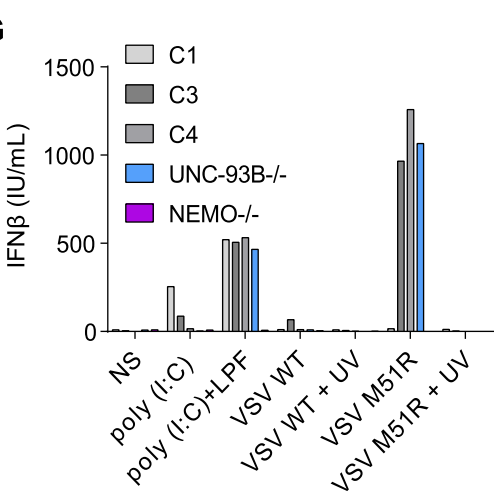
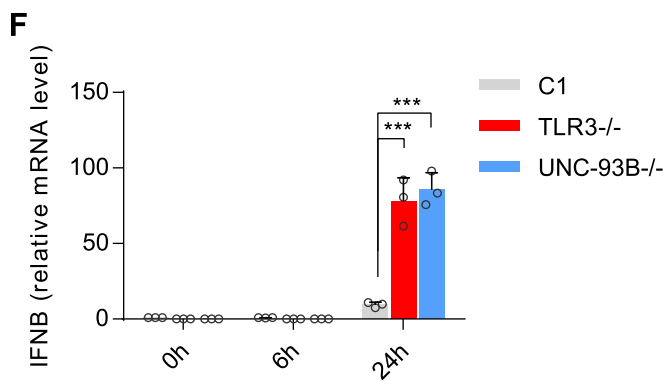
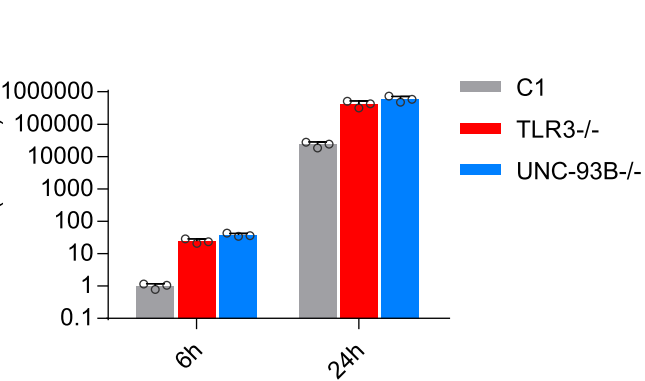
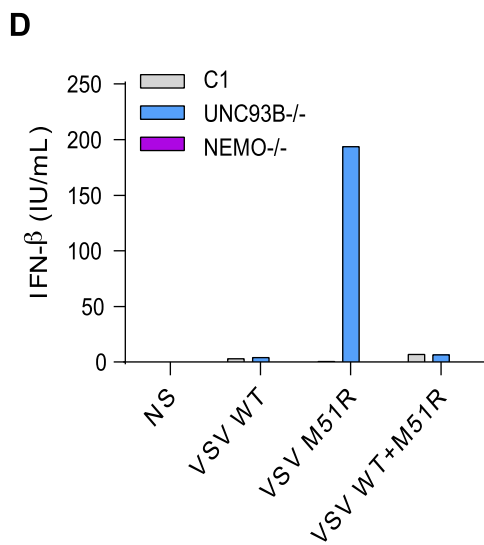
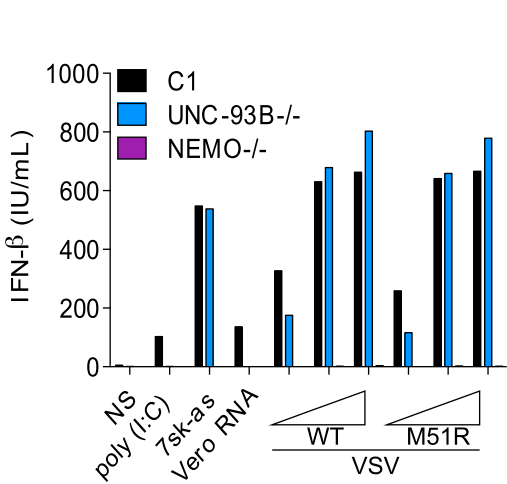
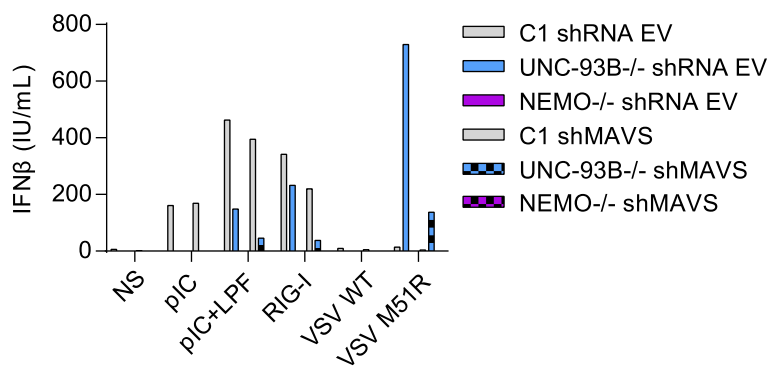
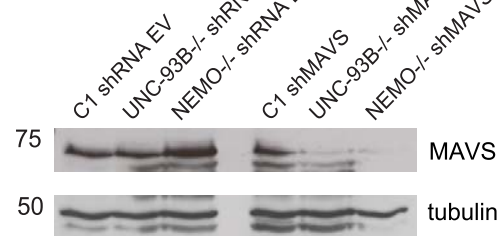
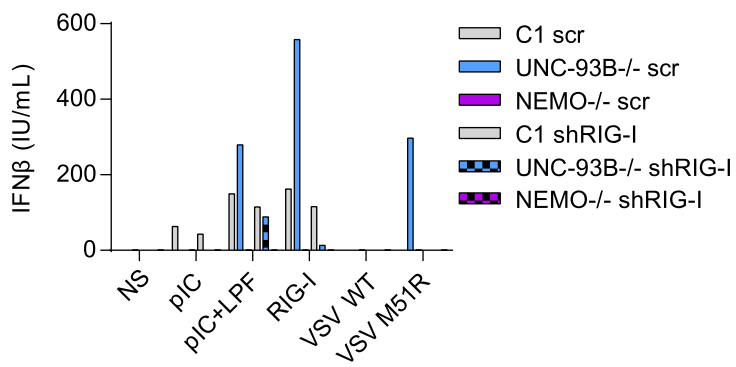
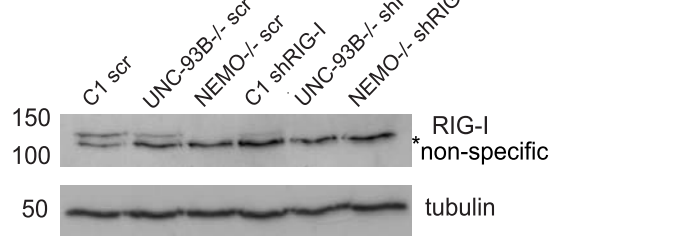
Gene ontology enrichment ( $p$ -value < 0.05) for the down- or upregulated differentially expressed ISGs common to TLR3<sup>-/-</sup>, STAT1<sup>-/-</sup> and TLR3 KO iPSC-derived cortical neurons.

**Figure S1**

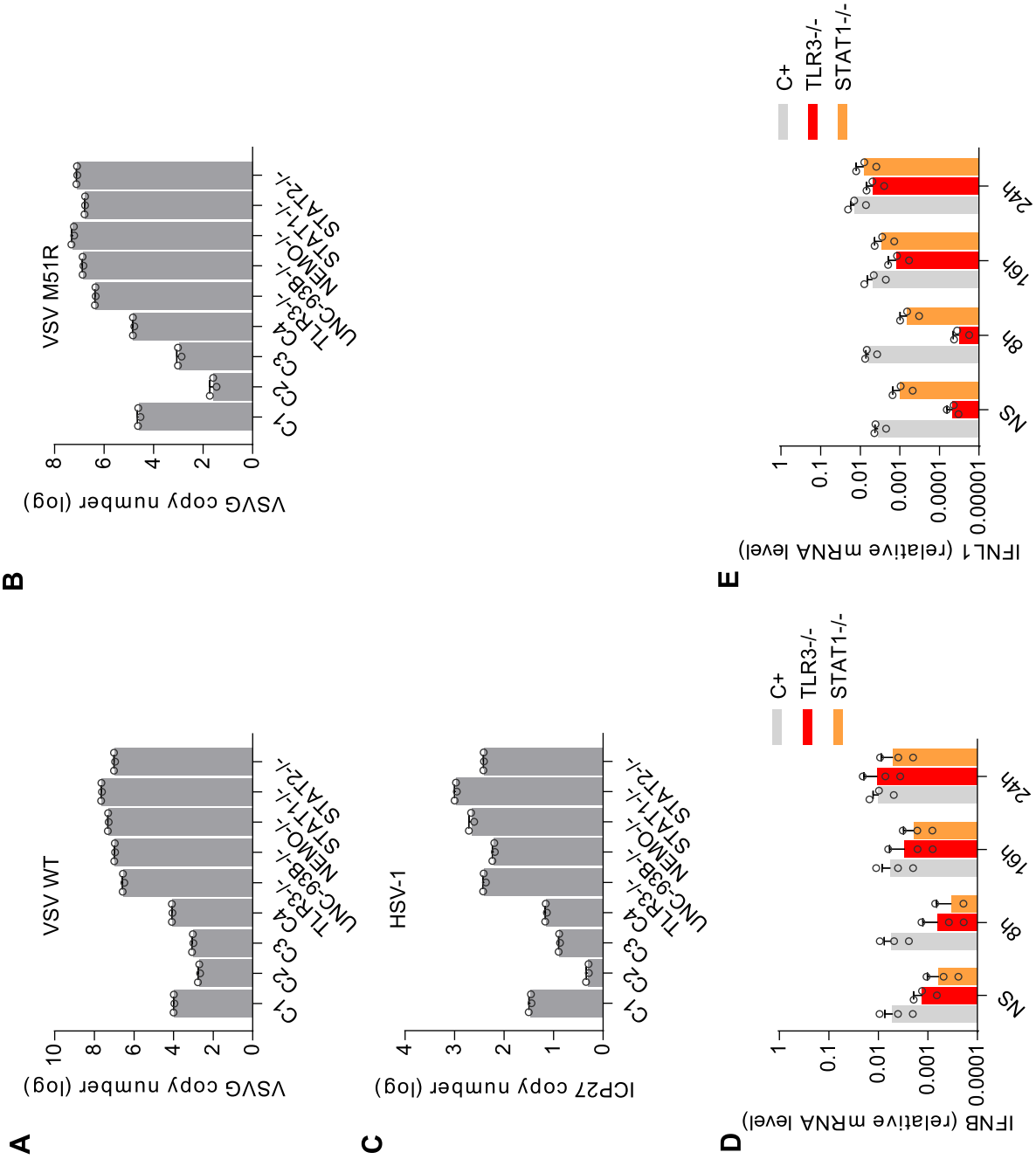


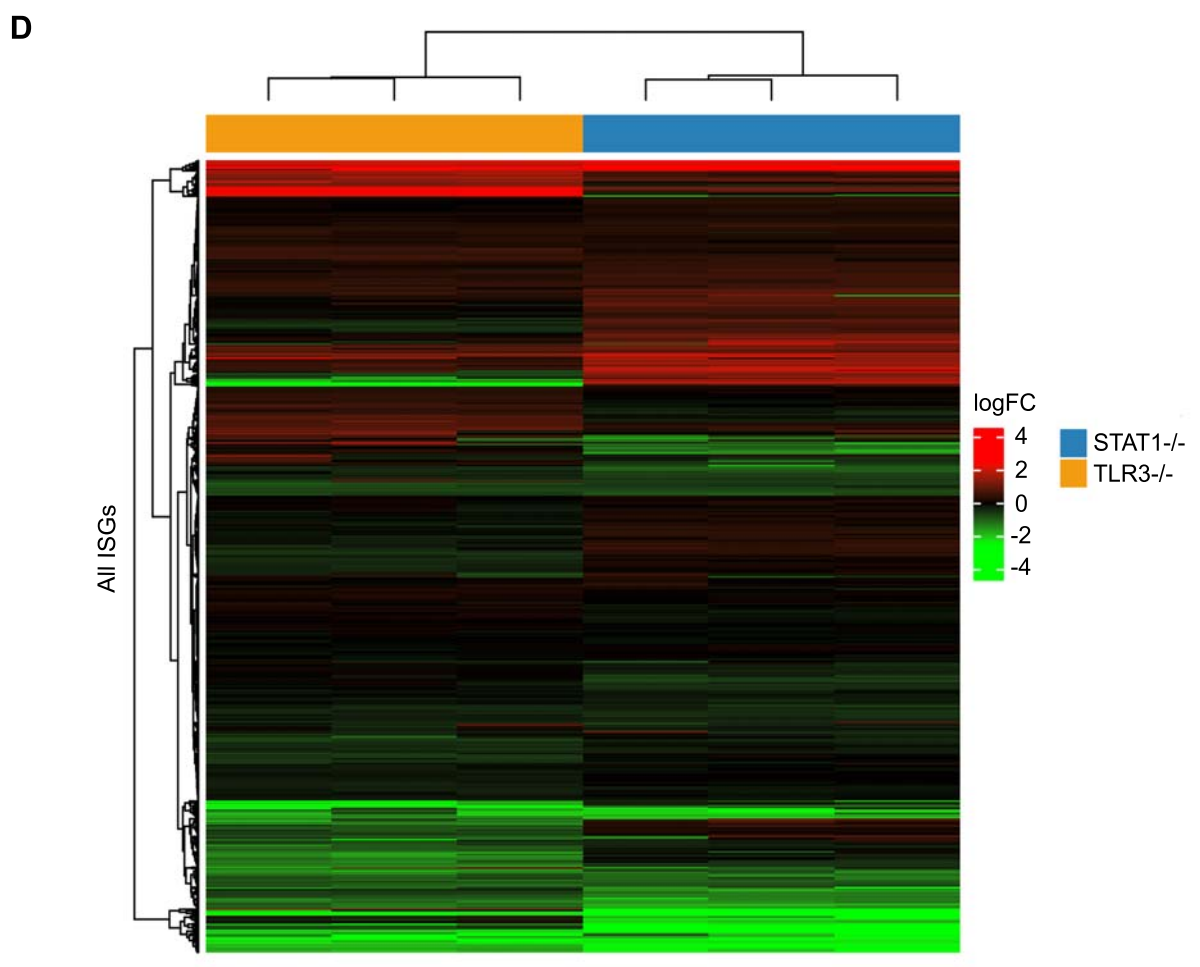
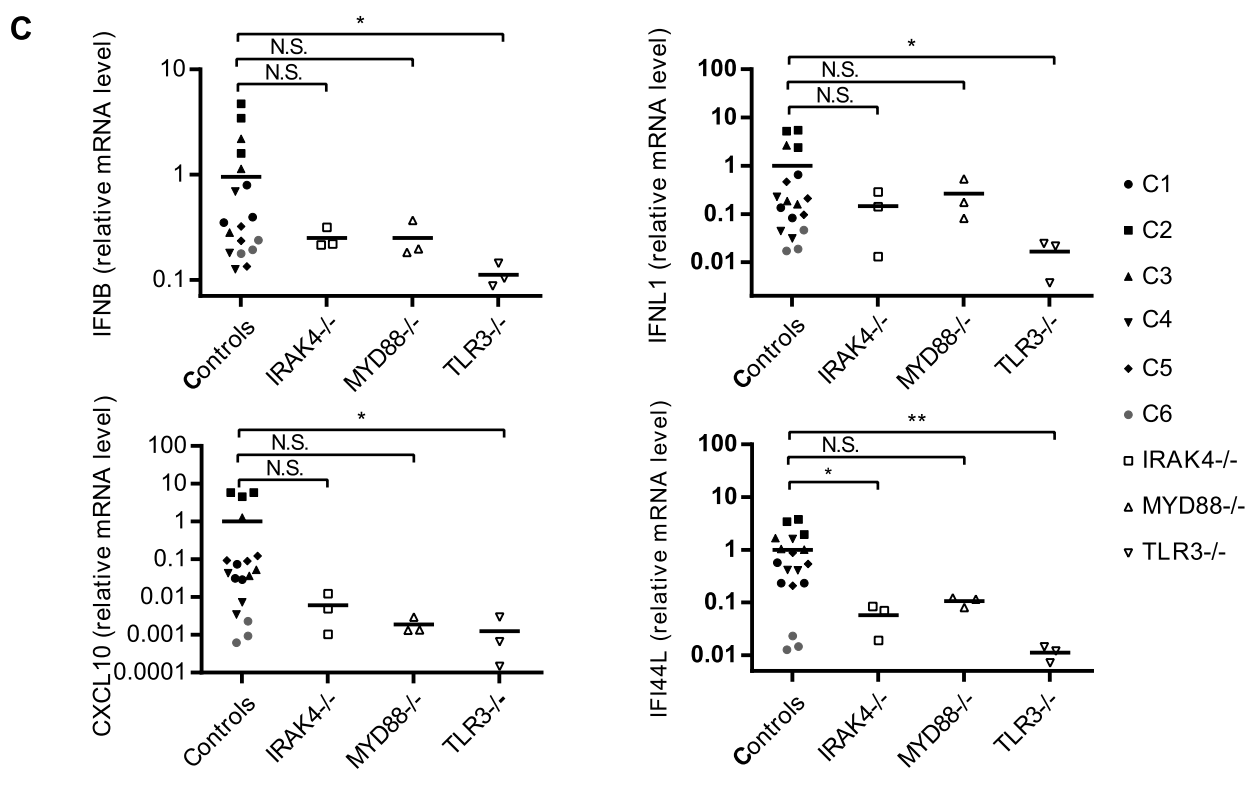
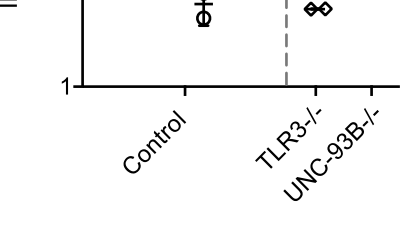
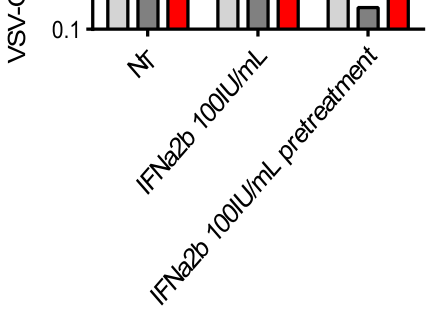
**Figure S2**

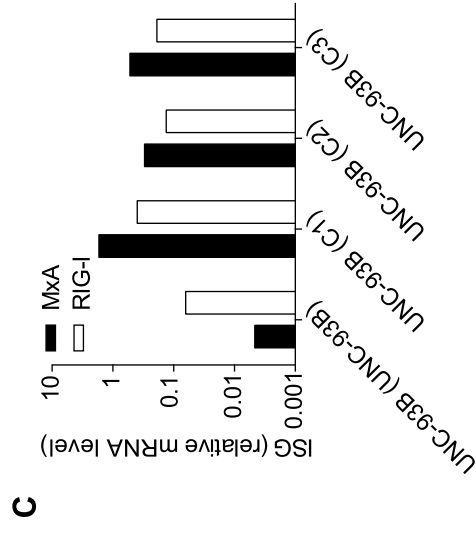
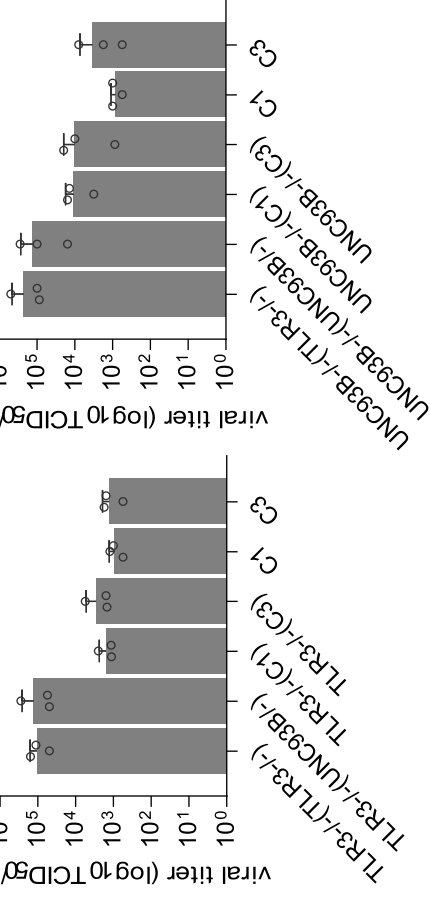
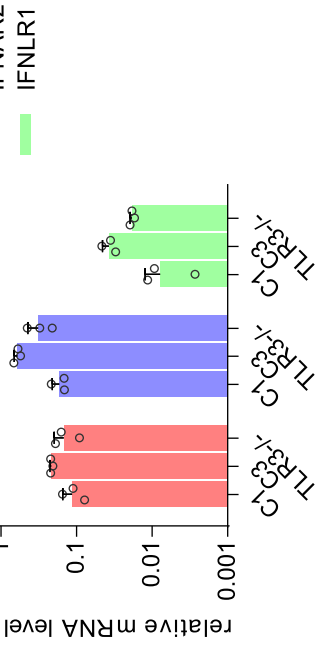




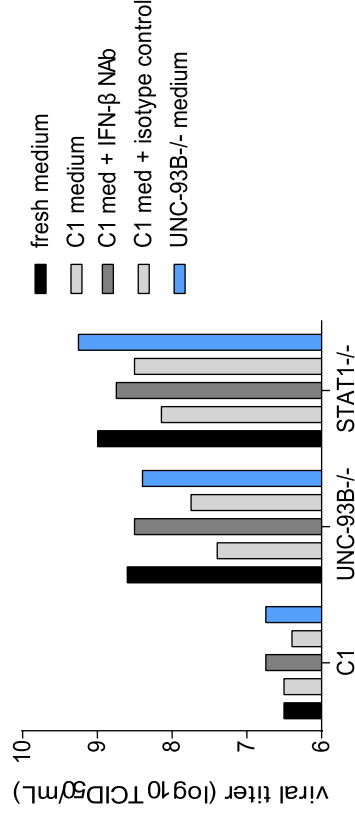
**Figure S4**



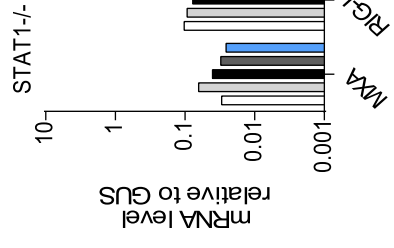
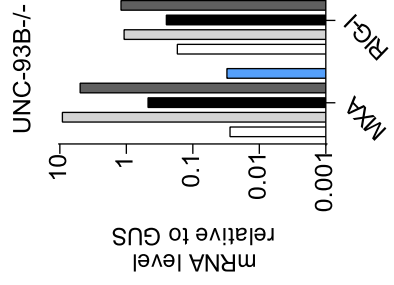
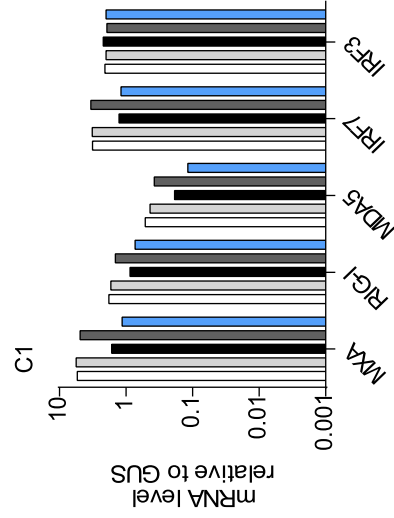




**D**



**E**



fresh medium

C1 medium

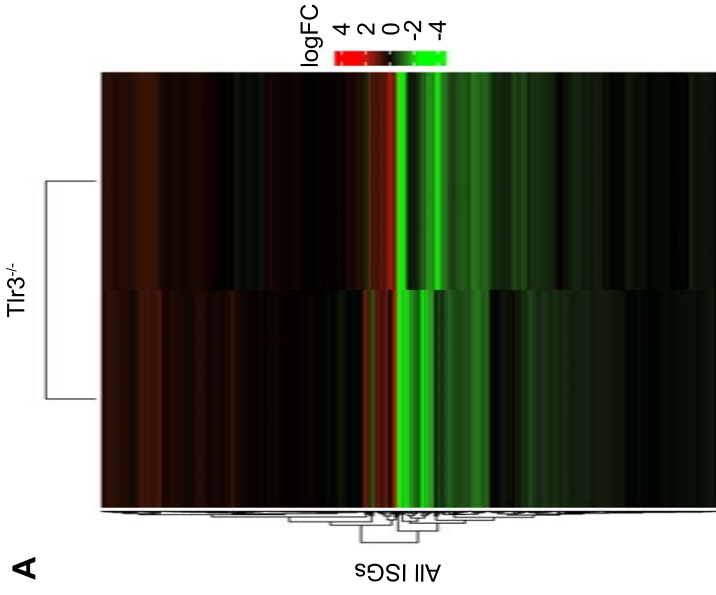
C1 med + IFN-β NAb

C1 med + isotype control

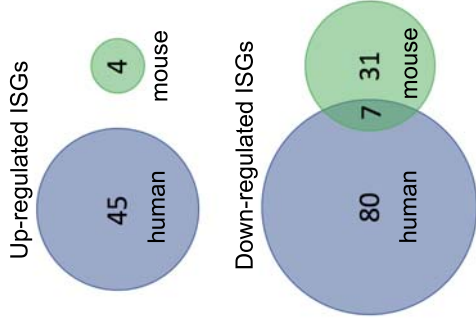
UNC-93B<sup>-/-</sup> medium

Figure S7

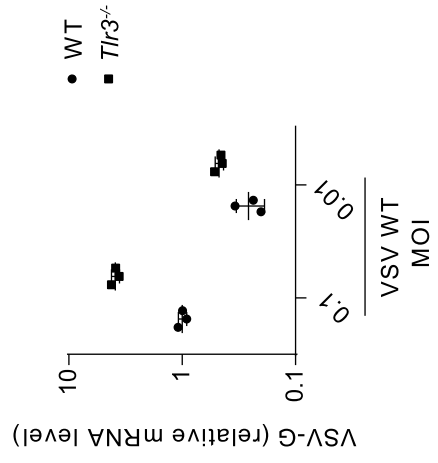
**A**



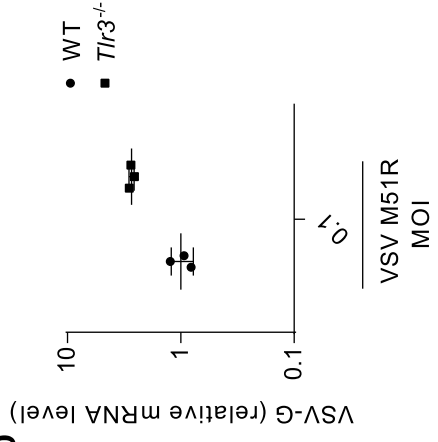
**B**



**C**



**D**



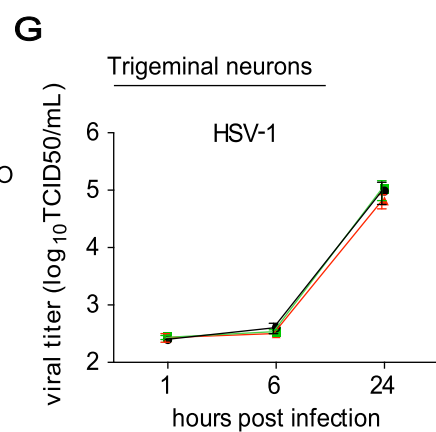
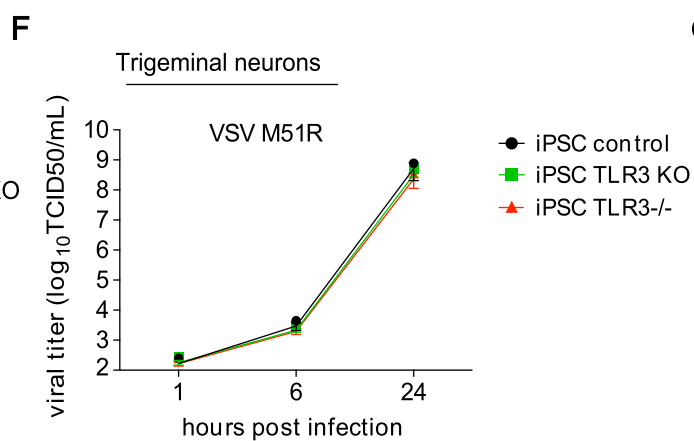
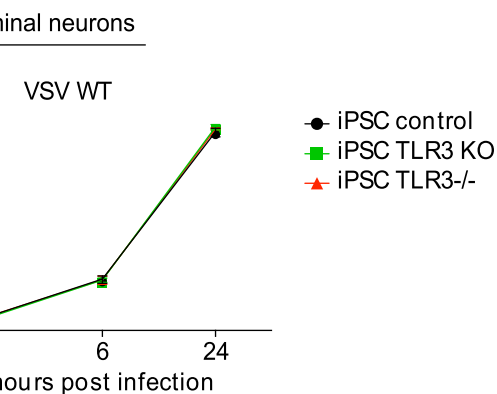
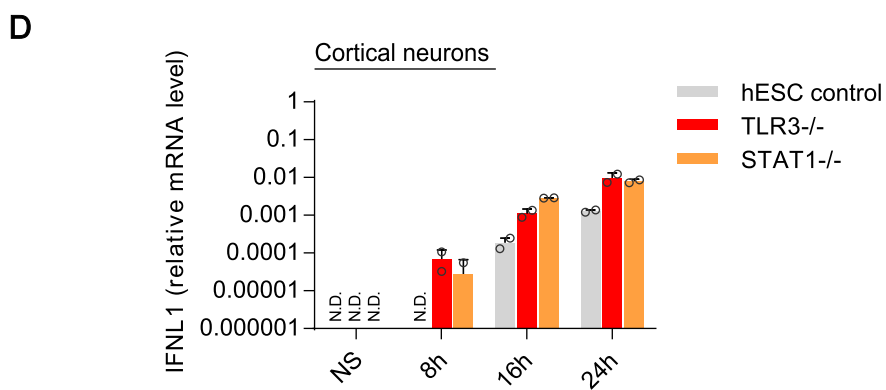
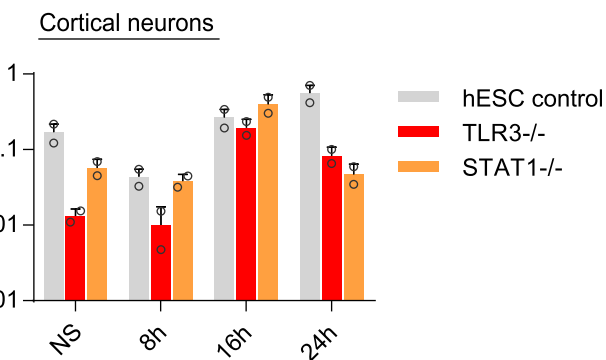
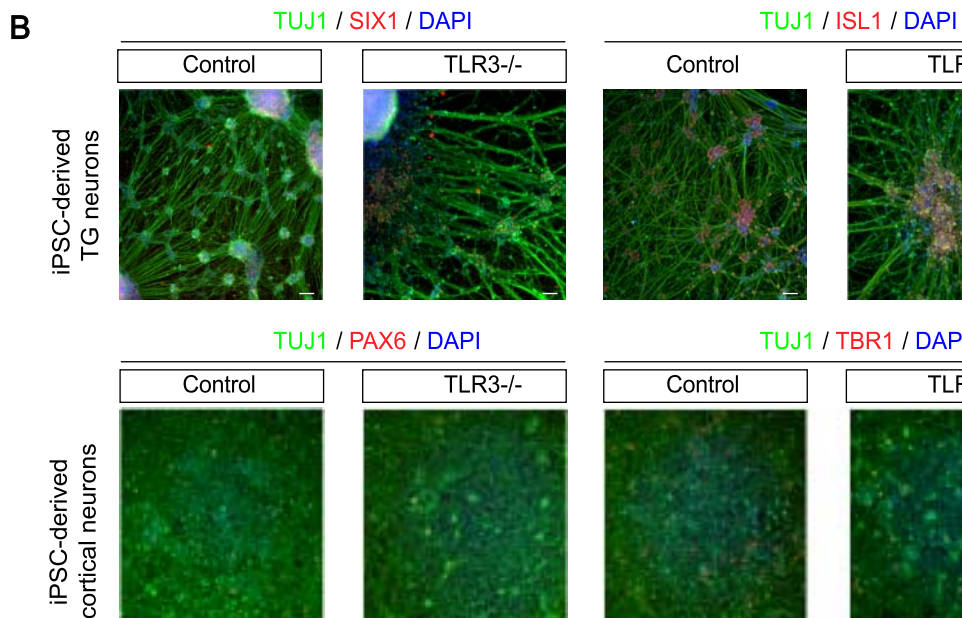
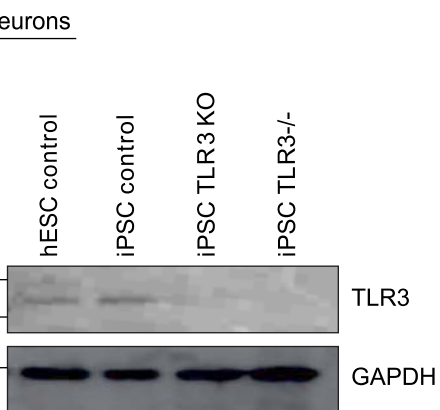


Figure S9

